Temperature and concentration dependences of Raman vibrational modes in $Rb_{1-x}(ND_4)_xD_2AsO_4$ mixed crystals

Chi-Shun Tu and Rong-Mei Chien
Department of Physics, Fu-Jen University, Taipei, Taiwan, Republic of China

V. Hugo Schmidt
Department of Physics, Montana State University, Bozeman, Montana 59717

(Received 8 August 1996)

The Raman vibrations ($10–10^3$ cm^{-1}) of A_1, B_2, and E symmetries along the [110] phonon direction have been measured as a function of temperature (80–293 K) in the mixed ferroelectric (FE) antiferroelectric system $Rb_{1-x}(ND_4)_xD_2AsO_4$ (DRADA-x) for ammonium concentrations $x=0$, 0.10, and 0.28. With decreasing temperature, the B_2 Raman shifts of RbD_2AsO_4 show both softening and hardening anomalies for four selected modes. In DRADA-0.10, the bending mode $\nu_2(B_2)$ (near 280 cm^{-1}) of the AsO_4 group exhibits a gradual softening down to $T\sim125$ K and then has a rapid drop. This phenomenon is attributed to a quick development of long-range FE ordering. In DRADA-0.28, the in-plane bending mode δ(O-D) (B_2) shows a softening near 220 K, whereas the bending mode $\nu_2(B_2)$ of the AsO_4 group exhibits a hardening. We associate these anomalies with the onset of glass formation. A doublet with splitting of about 10 cm^{-1} was observed in the ν_1 modes and was attributed to a slight deformation of the ν_1 vibration due to AsO_4 groups having different nearby ions (ND_4 and Rb). [S0163-1829(97)01605-6]

I. INTRODUCTION

Since the discovery that the deuterated family[1] with the formula $A_{1-x}(ND_4)_xD_2BO_4$ [A=Rb (or K) and B=P (or As)] exhibits a deuteron glass state for certain values of x, similar to the proton glass state observed in the undeuterated family,[2–5] many experimental techniques have been used in order to understand the nature of this deuterated family. In these systems, there is competition between the ferroelectric (FE) and the antiferroelectric (AFE) orderings, each characterized by specific configurations of the acid protons or deuterons. The random distribution of the Rb and ND_4 (or NH_4) ions produces frustration which can suppress the long-range electric order. Spontaneous polarization revealed that RbD_2AsO_4 (DRDA) has a first-order FE transition at $T_c\sim165$ K. Dielectric results indicated that at $T_m\sim146$ K, $Rb_{0.90}(ND_4)_{0.10}D_2AsO_4$ (DRADA-0.10) goes from the paraelectric (PE) to a PE/FE phase coexistence region, and then to another frequency-dependent coexistence (FE/deuteron glass) region at $T_g\sim60$ K ($f=0.05$ MHz).[6] Here T_m is the temperature that corresponds to the dielectric maximum. DRADA-0.28 has no FE phase, but has a frequency-dependent transition from the PE to the deuteron-glass phase at $T_g\sim65$ K ($f=0.1$ MHz). Field-heated, field-cooled, and zero-field-heated static permittivity also revealed that below $T_e\sim38$ K, the system enters a nonergodic state in which on practical time scales the acid deuterons of the O-D-···-O bonds cannot rearrange sufficiently to reach all energetically allowed configurations.[7]

DRADP-x mixed crystals in the concentration range $0.3\leqslant x\leqslant0.7$ have the KDP (KH_2PO_4)-type tetragonal symmetry (space group $I42d$-D_{2d}^{12}) down to liquid-He temperature with two formula units per primitive cell. According to the factor-group analysis for an ideal tetragonal KDP-type structure, both PO_4 and NH_4 tetrahedra have S_4 local site symmetry.[8] However, from investigations of Raman spectra of KDP and RbH_2PO_4, the local site symmetry of the PO_4 group was found to be C_2 in the paraelectric and ferroelectric phases.[9] In $NH_4H_2PO_4$, both PO_4 and NH_4 groups possess C_2 symmetry in the paraelectric phase and C_1 in the antiferroelectric phase.

In a KDP-type structure with S_4 site symmetry, the fully symmetric stretching vibration ν_1 of the PO_4 ion (free-ion value 980 cm^{-1})[10] should be observed only in the $A_1-y(zz)x$ geometry. At room temperature, this mode has frequency 882 cm^{-1} in DRADP-0.50 and 899 cm^{-1} in DRADP-0.48.[11,12] The doubly degenerate bending mode ν_2 of the PO_4 group (free-ion value 363 cm^{-1}) should be observed in the A_1, B_1, and B_2 Raman spectra. These main corresponding lines of the ν_2 mode were observed with the frequencies 352 (A_1) and 382 cm^{-1} (B_2) in DRADP-0.50, and 350 (A_1), and 379 cm^{-1} (B_2) in DRADP-0.48 at room temperature, respectively.[11,12]

The triply degenerate bending vibration ν_4 of the PO_4 group (free-ion value 515 cm^{-1}) should have a main component in both the B_1 and B_2 spectra and two components in the E spectrum. In the Raman spectra of DRADP-0.50, three lines (450, 510, and 542 cm^{-1}) in B_2 and two main peaks (476 and 530 cm^{-1}) in E were obtained at room temperature.[11] In DRADP-0.48, one B_2 line (490 cm^{-1}) and three E components (480, 526, and 551 cm^{-1}) were assigned at room temperature.[12] The region of asymmetric stretching mode ν_3 of the PO_4 group (free-ion value 1080 cm^{-1}) is the most difficult one to assign due to the possible overlap with the in-plane bending mode δ(O-D) and the ν_4 mode of the ND_4 group (free-ion value 1065 cm^{-1}).

In our earlier Brillouin scattering results along the [100] phonon direction, a broad damping peak which is stronger in

DRADA-0.28 was observed and was attributed to the fluctuations of local order parameter between FE and AFE phases.[13] The acoustic phonon frequency also shows a first-order hardening behavior as temperature decreases.[13] In the present paper, Raman scattering was carried out on the same samples (DRADA-$x=0$, 0.10, and 0.28) because Raman spectra can give important information including the glass formation that is usually associated with the local dynamic of the AsO_4 and ND_4 groups. Here, we pay special attention to the local environments and internal vibrations of the AsO_4 molecular group.

II. EXPERIMENTAL PROCEDURE

Single crystals of $Rb_{1-x}(ND_4)_xD_2AsO_4$ ($x=0$, 0.10, and 0.28) were grown from aqueous solutions with certain ratios of DRDA and $ND_4D_2AsO_4$ (DADA). The average size of these crystals is $1.2\times0.4\times0.2$ cm^3. The green light with $\lambda=514.5$ nm from an argon-ion laser was used as an excitation source. A double-grating monochromator (ISA Model U1000) equipped with a water cooled photomultiplier tube detector was used. The scanning operation was chosen with resolution 1 cm^{-1} and slits: 200/400/400/200 (μm). Right-angle spectra were taken from scattering geometries $y(zz)x$, $y(xz)x$, and $y(xy)x$ which correspond to A_1, E, and B_2 symmetries, respectively. Here x, y, and z correspond to the crystal a, b, and c axes, respectively. A Janis VPF-100 variable temperature pourfill cryostat was used with a Lake-Shore 321 temperature controller. The samples were heated from 80 K up to room temperature by steps. The data were collected automatically using a microcomputer, and the accumulated time for each scan is about 40 min. Results were found to be reproducible for all compounds. Here the Lorentz profile was used to fit the Raman spectra, from which the Raman frequency shifts for various modes were obtained.

III. RESULTS AND DISCUSSION

By a group-theory analysis for the KDP type structure (which contains two molecular units of KH_2PO_4 in a primitive unit cell); at zero wave vector, the vibrational modes in the tetragonal symmetry (space group $I\bar{4}2d$-D_{2d}^{12}) can be decomposed into the following irreducible representations:[14,15]

$$\Gamma_{\text{vib}}=4A_1(R)+5A_2\ \ (\text{silent})\ \ +6B_1(R)+6B_2(R,IR)+12E(R,IR). \tag{1}$$

The symmetry species A_1, B_1, B_2, and E are Raman active. The situation in mixed crystals DRADP and DRADA is more complicated than in the parent compounds, because some Rb atoms have been substituted by ND_4 groups. In this case, the selection rule is expected to be broken much more easily than in the pure compounds. The local site symmetries of the AsO_4 and ND_4 groups are also anticipated to be lower as compared with the parent crystals.

In this work, the A_1 Raman spectra show a similar pattern to the one in DRADP-0.48. Thus, the assignments of vibrational modes corresponding to the A_1 symmetry were made first in accordance with the A_1 spectra of DRADP-0.48.[12] In DRADA-x, each corresponding line of the A_1 symmetry shows lower frequency and can be attributed to the heavier arsenic atom. The various vibrations of the B_2 and E symmetries were assigned by comparing with the A_1 modes.

A. Temperature-dependent B_2 $y(xy)x$ modes

Actual temperature-dependent B_2 Raman spectra are shown in Figs. 1(a)–1(c) for $x=0$, 0.10, and 0.28, respectively. The three compounds display a similar Raman pattern except for the low-temperature spectra of DRDA. Frequencies near 300 and 800 cm^{-1} also demonstrate a high scattering efficiency that is associated with the optical nonlinearity. The main lines observed from this configuration are at frequencies near 300, 360, 760, and 820 cm^{-1}.

The temperature dependences of four selected B_2 modes for each compound are plotted in Figs. 2(a)–2(c). The highest-frequency mode (near 820 cm^{-1}) corresponds to the in-plane bending mode δ(O-D). Modes around 760 and 360 cm^{-1} belong to the stretching mode ν_1 and the bending mode ν_4 of the AsO_4 group, respectively. Those frequencies located near 280 and 300 cm^{-1} are associated with the bending mode ν_2 of the AsO_4 group. In DRDA, both the δ(O-D) and ν_4 bending modes show apparent step-up (hardening) anomalies at $T_c\sim160$ K as temperature decreases. The changes of the δ(O-D) and ν_4 modes above and below T_c are about 4 cm^{-1} (0.5%) and 4 cm^{-1} (1.1%), respectively. On the contrary, the ν_1 and ν_2 vibrations of the AsO_4 group display step-down (softening) behaviors with frequency reductions 5 cm^{-1} (0.6%) for ν_1 and 13 cm^{-1} (5%) for ν_2. These phenomena confirm that the pure DRDA crystal possesses a ferroelectric transition in the temperature domain.

For DRADA-0.10, the bending mode ν_2 (near 280 cm^{-1}) of the AsO_4 group exhibits a gradual softening as temperature decreases down to $T\sim125$ K and then has a rapid drop. What are the origins of this phenomenon? The ND_4^+ deuteron NMR spectra[16] of DRADA-0.10 showed a progressive disappearance of the doublet near 130 K, from which it was concluded that below 130 K the FE phase portion is greater than the PE portion in the crystal and becomes the dominant ordering. This result is consistent with the presence of PE/FE phase coexistence as evidenced by dielectric results which show that a gradual ferroelectric transition begins at $T_m=146$ K and is mostly completed at ~120 K.[6] In addition, the acoustic phonon damping also shows a sharp peak near 130 K which was attributed to a rapid growth of FE ordering.[13] Consequently, one can conclude that the slow softening (shown in ν_2 mode) beginning from room temperature must relate to the freezing-in of the ND_4 reorientations which increases the local structural competition, and eventually the FE phase becomes the governing ordering near $T\sim125$ K.

As shown in Fig. 2(c) for DRADA-0.28, a softening near 220 K has been observed in the in-plane bending mode δ(O-D) (near 815 cm^{-1}) as temperature decreases, whereas the bending mode ν_2 (near 300 cm^{-1}) of the AsO_4 group exhibits a hardening behavior. The frequencies of both the ν_2 and δ(O-D) modes are sensitive to the deuteron ordering near the AsO_4 group. If the deuteron arrangement varies with the temperature, the mass and the force constants of the D_2AsO_4 group will change and thus influence the frequencies of the ν_2 and δ(O-D) modes. It is reasonable to connect

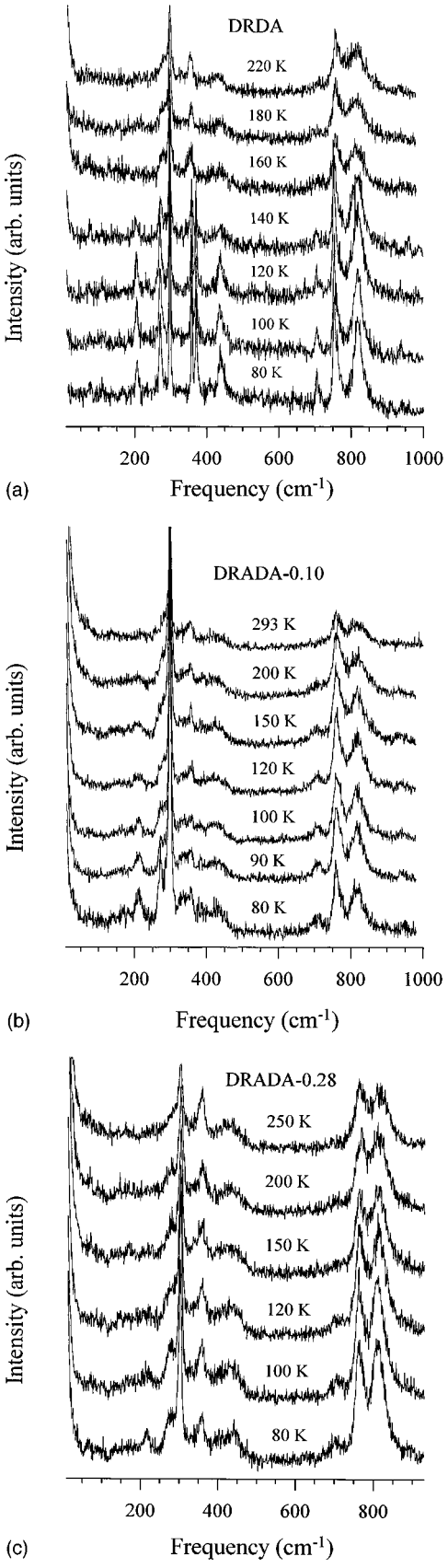

FIG. 1. Temperature dependence of Raman spectra of (a) DRDA, (b) DRADA-0.10, and (c) DRADA-0.28 measured from the $y(xy)x$ geometry between 10–1000 cm^{-1}. Here the Raman vibrations correspond to the B_2 symmetry.

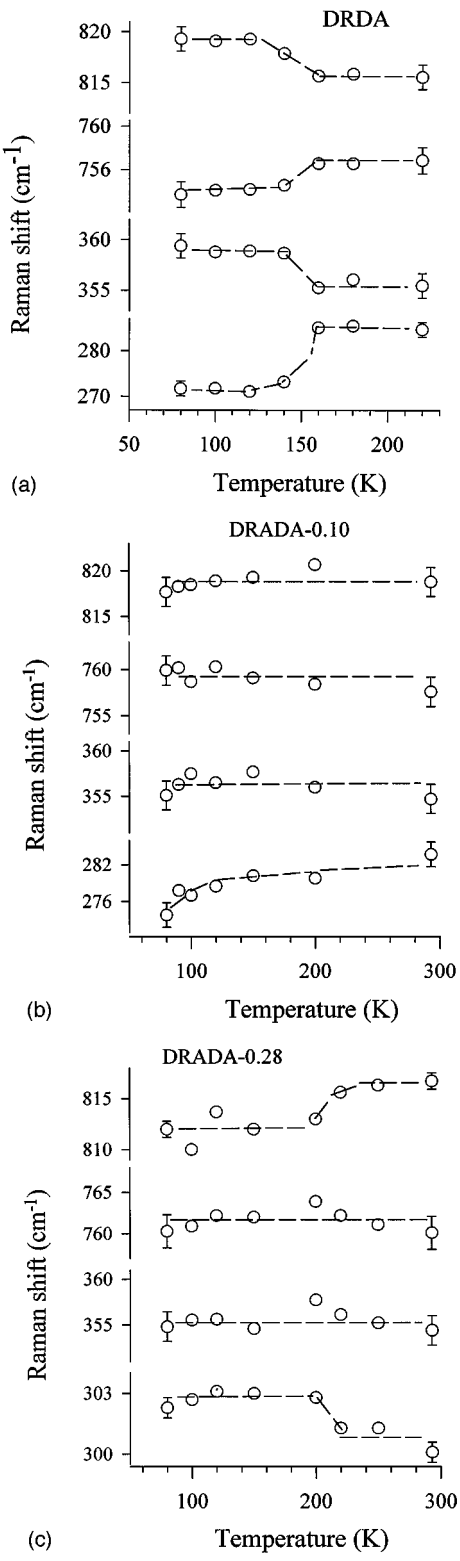

FIG. 2. Frequency vs temperature variations of four selected modes (with B_2 symmetry) of (a) DRDA, (b) DRADA-0.10, and (c) DRADA-0.28. These four modes correspond to the in-plane bending mode δ(O-D) (near 820 cm^{-1}), stretching mode ν_1 (near 760 cm^{-1}), and bending modes ν_4 (near 360 cm^{-1}) and ν_2 (near 280 and 300 cm^{-1}). Here ν_1, ν_2, and ν_4 are the internal vibrations of the AsO_4 group. The dashed lines are guides for the eye.

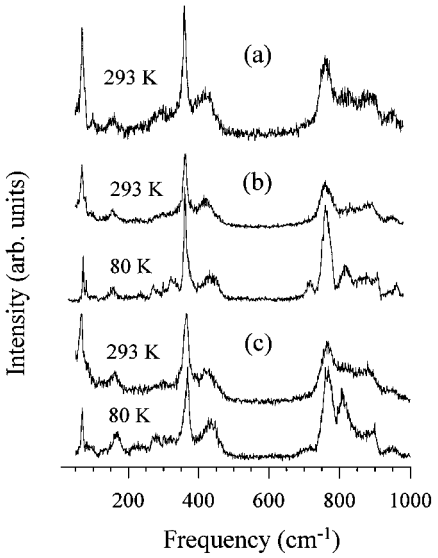

FIG. 3. Raman components of the $E-y(xz)x$ symmetry of (a) DRDA, (b) DRADA-0.10, and (c) DRADA-0.28 measured at two different temperatures (80 and 293 K).

these two breaks at approximate 220 K with the temperature of onset of glass formation. A similar phenomenon was also observed in the ν_2 (B_2) mode of the PO_4 group of DRADP-0.48, in which the onset temperature of glass formation is ~ 200 K.

B. Comparison of A_1, B_2, and E symmetries

The right-angle spectra from scattering geometries $A_1-y(zz)x$ and $E-y(xz)x$ are given in Figs. 3 and 4 at two different temperatures where the samples possess tetragonal structure. Here we do not show the Raman spectrum of DRDA at $T=80$ K because the DRDA crystal becomes orthorhombic with space group C_{2v}^{19} ($Fdd2$) below T_c. The

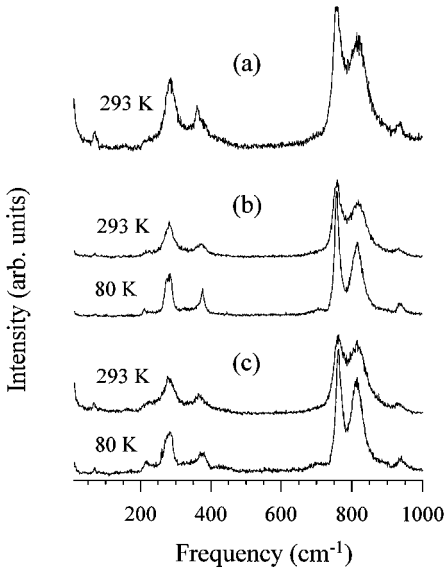

FIG. 4. Raman components of the $A_1-y(zz)x$ symmetry of (a) DRDA, (b) DRADA-0.10, and (c) DRADA-0.28 measured at two different temperatures (80 and 293 K).

TABLE I. Frequencies of observed Raman modes (in cm^{-1}) in DRADA-x (*, $x=0$; +, $x=0.10$; and ++, $x=0.28$).

$T=80$ K			$T=293$ K			
(B_2) $y(xy)x$	(E) $y(xz)x$	(A_1) $y(zz)x$	(B_2) $y(xy)x$	(E) $y(xz)x$	(A_1) $y(zz)x$	Assignments
	72^{+} 99^{+} 69^{++} 90^{++}	70^{+} 69^{++}		70* 100* 69^{+} 96^{+} 65^{++}	71* 70^{+} 67^{++}	External modes
168^{+}	157^{+} 167^{++}	171^{++}		156* 156^{+} 159^{++}	157* 163^{++}	AsO_4 libration
211^{+} 213^{++}		216^{+} 218^{++}			221* 215^{+} 224^{++}	ND_4 libration
274^{+} 299^{+} 276^{++} 302^{++}	275^{+} 325^{+} 276^{++}	274^{+} 286^{+} 277^{++} 288^{++}	281^{+} 299^{+} 274^{++} 300^{++}	309* 321^{+} 298^{++}	283* 293* 276^{+} 283^{+} 281^{++} 291^{++}	ν_2 of AsO_4
331^{+} 355^{+} 423^{+} 355^{++} 433^{++}	365^{+} 440^{+} 368^{++} 434^{++}	352^{+} 377^{+} 372^{++}	330^{+} 355^{+} 423^{+} 354^{++} 425^{++}	361* 363^{+} 422^{+} 365^{++} 426^{++}	367* 372* 377^{+} 368^{++}	ν_4 of AsO_4
706^{+} 760^{+} 775^{+} 700^{++} 764^{++} 772^{++}	714^{+} 761^{+} 774^{+} 694^{++} 760^{++} 773^{++}	758^{+} 766^{+} 762^{++} 772^{++}	758^{+} 773^{+} 760^{++} 767^{++}	760* 757^{+} 773^{+} 765^{++}	756* 768* 756^{+} 766^{+} 758^{++} 769^{++}	ν_1 of AsO_4
818^{+} 812^{++}	818^{+} 813^{++}	816^{+} 814^{++}	819^{+} 817^{++}	823* 834^{+} 821^{++}	818* 819^{+} 816^{++}	δ (O-D)
	962^{+} 960^{++}	938^{+} 939^{++}		955* 953^{+} 953^{++}	938* 934^{+} 934^{++}	ν_3 of AsO_4

main vibrational frequencies of the B_2, A_1, and E symmetries observed at two different temperature ($T=80$ and 293 K) are summarized in Table I.

As mentioned earlier, the symmetric stretching mode ν_1 of the AsO_4 group is nondegenerate with only A_1 symmetry. However, as shown in Figs. 1 and 3 and Table I, the leakage of the ν_1 mode into the E and B_2 symmetries is practically as strong as the other permitted vibrations. The ν_1 leakage that occurs in both the E and B_2 configurations is possible as the result of the lowering of local symmetry of the AsO_4 groups from S_4 to C_2 or even to C_1. The degree of the ν_1 leakage also is stronger as compared with the partially deuterated DRADP-0.48 crystal and may imply that the local symmetry

of the AsO_4 group in the DRADA-x (0, 0.10, and 0.28) system is lower than that of the PO_4 group in the DRADP system. While comparing the relative intensity of the ν_1 mode with other vibrations, one can note that the ν_1 leakage increases with increasing ammonium concentration x. This may occur because the partial substitution of Rb ions by ND_4 ions will lower the local symmetry of the AsO_4 group. Another interesting feature is that a frequency doublet with a narrow splitting of about 10 cm^{-1} was observed in the ν_1 mode. This property occurs in the A_1, B_2, and E geometries for all three samples. A possible reason for this splitting is that different AsO_4 groups have different combinations of surrounding ions (ND_4 and Rb), which will cause slight perturbation to the ν_1 frequency.

The doubly degenerate bending mode ν_2 should be observed in the A_1 and B_2 modes if the AsO_4 group has an S_4 site symmetry. As given in Table I for $T=80$ K, the ν_2 mode at 274 cm^{-1} (A_1) in $x=0.10$ and 277 cm^{-1} (A_1) in $x=0.28$, also show symmetry leakage into the E and B_2 geometries.

The triply degenerate bending mode ν_4 should have a main Raman component in the B_2 symmetry and two components in the E symmetry. This mode, owing to its character associated with the deuteron (or proton) collective motions in the c plane, is sensitive to the existence of additional D bonds. At $T=80$ K, two strong peaks at 365 and 440 cm^{-1} in $x=0.10$, and 368 and 434 cm^{-1} in $x=0.28$ were observed in the E symmetry. For the B_2 symmetry, there are three Raman lines (331, 335, and 423 cm^{-1}) in $x=0.10$ and two components (355 and 433 cm^{-1}) in $x=0.28$.

The antisymmetric stretching mode ν_3 is difficult to assign because both the in-plane bending mode δ(O-D) and the ν_4 mode of the ND_4 ion appear also in this frequency range. Those values of the δ(O-D) and ν_3 modes of the AsO_4 group given in Table I were assigned in accordance with the A_1 Raman components of DRADP-0.48.

With the results of Yuzyuk *et al.*[11] (for DRADP-0.50) and Martinez, Agullo-Rueda, and Schmidt[12] (for DRADP-0.48), we assign frequencies located at ranges 150–175 and 210–230 cm^{-1} to the librations of the arsenate and ammonium groups, respectively. The Raman components with frequency below 100 cm^{-1} were assigned to the external vibrations associated with the Rb and ND_4 ion motions.

IV. CONCLUSIONS

The mixed crystals DRADA-x (0, 0.10, and 0.28) display similar Raman spectra for Raman active species (A_1, B_2, and E) and indicate a strong symmetry leakage possibly due to the lowering of local site symmetry of the AsO_4 group from S_4 to C_2 (or even C_1). The temperature-dependent Raman shifts of the pure DRDA crystal show both step-down (softening) and step-up (hardening) anomalies at $T_c \sim 160$ K. This is consistent with our previous Brillouin scattering results in which a first-order transition occurs. For DRADA-0.10, the bending mode ν_2 (near 280 cm^{-1}) of the AsO_4 group exhibits a gradually softening down to $T \sim 125$ K, and then has a rapid drop. This behavior confirms a rapid growth of long-range FE ordering at $T \sim 125$ K as concluded in our earlier Brillouin results. In DRADA-0.28, with temperature decreasing, both softening and hardening near 220 K were also observed in the in-plane bending mode δ(O-D) and ν_2 mode of the AsO_4 group, respectively. We connect this high-temperature anomaly with the onset of deuteron glass behavior.

The assignments of various Raman-active modes (corresponding to A_1, B_2, and E symmetries) in DRADA-x (0, 0.10, and 0.28) have been made in accordance with the A_1 Raman spectrum of the DRADP-0.48 crystal. The ν_1 (A_1) mode exhibits a frequency doublet with splitting of about 10 cm^{-1}. It was attributed to the slight deformation of the ν_1 vibration due to the fact that different AsO_4 groups have different environments depending on the identity of the attaching groups (ND_4 and Rb ions).

ACKNOWLEDGMENTS

The authors express sincere thanks to Dr. L.-G. Hwa for use of the Raman scattering facility, to Shi-Shan Gao for helpful assistance in measurement, and to Dr. N. J. Pinto for crystals. This work was supported in part by NSF Grant No. DMR-9520251 and DOE Equipment Grant No. FG05-91ER79046.

[1] V. H. Schmidt, S. Waplak, S. Hutton, and P. Schnackenberg, Phys. Rev. B **30**, 2795 (1984).
[2] E. Courtens, J. Phys. Lett. (Paris) **43**, L199 (1982).
[3] Z. Trybula, V. H. Schmidt, J. E. Drumheller, D. He, and Z. Li, Phys. Rev. B **40**, 5289 (1989).
[4] C.-S. Tu, V. H. Schmidt, and A. A. Saleh, Phys. Rev. B **48**, 12 483 (1993).
[5] F. L. Howell, N. J. Pinto, and V. H. Schmidt, Phys. Rev. B **46**, 13 762 (1992).
[6] N. J. Pinto, Ph.D. thesis, Montana State University, 1992.
[7] N. J. Pinto, K. Ravindran, and V. H. Schmidt, Phys. Rev. B **48**, 3090 (1993).
[8] E. Courtens and H. Vogt, J. Chim. Phys. **82**, 317 (1985).
[9] Y. Tominage, Ferroelectrics **52**, 91 (1983).
[10] G. Herzberg, *Infrared and Raman Spectra of Polyatomic Molecules* (Van Nostrand, Princeton, NJ, 1945).
[11] Y. I. Yuzyuk, I. Gregora, V. Vorlicek, J. Pokorny, and J. Petzelt, J. Phys. Condens. Matter **7**, 683 (1995).
[12] J. L. Martinez, F. Agullo-Rueda, and V. H. Schmidt, Ferroelectrics **76**, 23 (1987).
[13] C.-S. Tu and V. H. Schmidt, Phys. Rev. B **50**, 16 167 (1994).
[14] M. S. Shur, Kristallografiya **11**, 448 (1966) [Sov. Phys. Crystallog. **11**, 394 (1966)].
[15] M. Kasahara, M. Tokunaga, and I. Tatsuzaki, J. Phys. Soc. Jpn. **55**, 367 (1986); **55**, 2477 (1986).
[16] N. J. Pinto, F. L. Howell, and V. H. Schmidt, Phys. Rev. B **48**, 5983 (1993).